

Examination of a density current with severe winds and extensive dust: South Australia case study 2 April 2005

Belinda Gibson

Regional Office, Bureau of Meteorology, Adelaide, Australia

(Manuscript received March 2007; revised August 2007)

On 2 April 2005 a density current formed along a pre-frontal trough and progressed eastwards across South Australia. Record high April temperatures were experienced ahead of the trough, with severe wind gusts recorded across many parts of the State as winds shifted from northwesterly to southwesterly. An extensive area of dust accompanied the density current, producing significant reductions in visibility in its wake. One-minute data from the Royal Australian Air Force (RAAF) Base Edinburgh were used to examine the properties of the density current including its height, propagation speed, temperature profile and effect on wind speed. A periodicity in the wind, pressure and visibility was observed, varying according to the Brunt-Väisälä frequency. These oscillations were indicative of internal gravity waves at the head of the density current propagating in the opposite direction to the surface wind.

Introduction

A pre-frontal trough developed ahead of a cold front near the western border of South Australia during the morning of 2 April 2005. Ahead of the trough, conditions were hot and clear, with record high April temperatures and falling pressures. The trough advanced rapidly eastward during the day bringing a marked drop in temperature, an increase in humidity and sharp pressure rises. Winds shifted from the northwest to the southwest with the passage of the trough, with severe wind gusts recorded across many parts of the State. An extensive area of dust was observed in the cooler, southwest airstream bringing significant

and sustained reductions in visibility. The trough represented the main change of the day, with little further change in temperature or wind strength associated with the cold front, signifying that frontogenesis had occurred along the pre-frontal trough. It is noted, however, that in order to distinguish between the two features, the terms trough and pre-frontal trough are used to describe the first feature, even after it had developed into the main change.

The trough marked the boundary between two distinct air masses such that the passage of the trough could be considered in terms of a density current where a colder, denser air mass entered into and displaced a pre-existing environment. It was therefore possible to apply density current theory to the rate of movement of the trough, with the calculated propagation speed comparing favourably to that observed. The height of the density current was also determined,

Corresponding author address: Belinda Gibson, Bureau of Meteorology, PO Box 421, Kent Town, South Australia 5071, Australia.
Email: b.gibson@bom.gov.au

giving an indication of the vertical extent of the dust.

An extremely large horizontal pressure gradient was found to exist across the leading edge of the density current, with a sudden peak in pressure with the density current's arrival. This was shown to produce a local acceleration in the wind speed through momentum changes associated with the change in air mass. Inspection of one-minute data of wind, visibility and pressure showed a periodicity in the values varying according to the Brunt-Väisälä frequency. The observed oscillations and the relationship between the three elements indicated the existence of internal gravity waves at the head of the density current propagating against the flow of the surface wind.

In subsequent sections of this study an overview of the meteorological situation is provided and the mechanism through which the trough developed into a density current is outlined. Statewide observations of the pre and post-trough environment are described, before particular attention is given to the high-resolution data from Edinburgh RAAF Base to make a close examination of the density current. Details of the season-to-date rainfall are then presented as an important precursor to the dust event. The impact of the event across South Australia is then addressed, followed by consideration of numerical weather prediction. The final two sections outline future directions and provide a summary of the event.

Meteorological situation

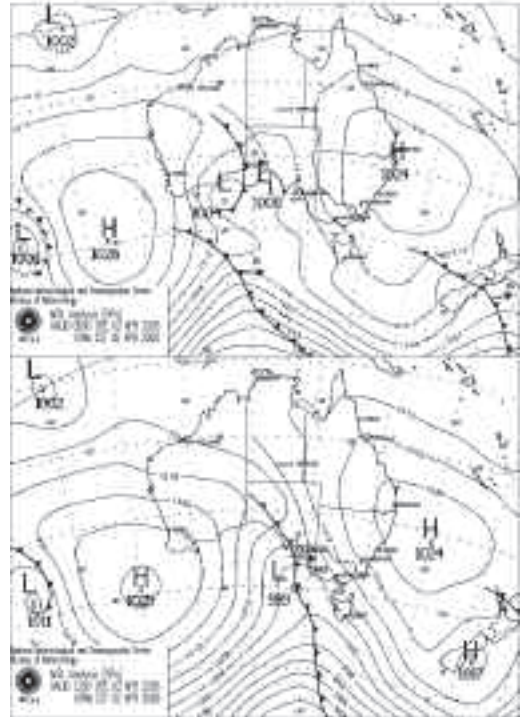
Note: Central Standard Time = UTC + 9.5 hours.

The mean sea-level pressure analyses for 0000 UTC and 1200 UTC 2 April 2005 are given in Fig. 1. The charts show a cold front and associated low pressure system near the western border of South Australia at 0000 UTC with a pre-frontal trough over the west of the State. The system moved rapidly eastward during the day with the trough having reached the eastern districts of South Australia by 1200 UTC.

A northerly airstream extended across South Australia ahead of the trough, with clear skies and hot conditions. Many sites experienced record high maximum temperatures for April, with temperatures typically 12 to 15 degrees above the 2 April average. The passage of the trough was marked by a sudden backing of the winds to the west-southwest and the arrival of cooler, denser air and sharp pressure rises.

Winds remained from the southwest for four to six hours following the passage of the trough before veering to the northwest again. Middle-level cloud gradually increased ahead of the front bringing first virga and then rain, similarly some four to six hours following the initial wind change.

Fig. 1 Mean sea-level pressure analyses, (a) 0000 UTC and (b) 1200 UTC 2 April 2005.

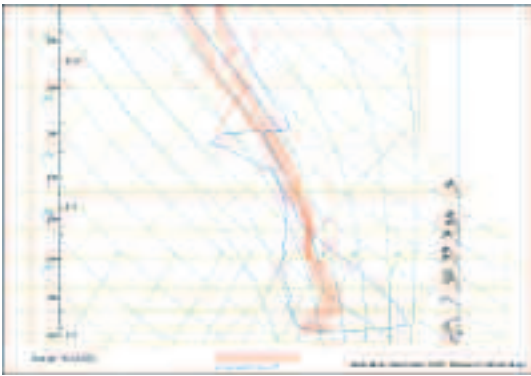


Development of the trough and density current

The 1800 UTC 1 April 2005 mean sea-level pressure analysis (not shown) indicated a cold front over the south of Western Australia with a pre-frontal trough near the western border of South Australia to the west of Nullarbor. Little change was observed in the position of this trough on the 2100 UTC analysis. Middle-level cloud extended eastwards ahead of the trough with a more consolidated cloudband with areas of rain to the west of the trough.

By 2300 UTC the trough had moved east through Nullarbor with the rain increasing in the west. Eucla, approximately 10 km west of the South Australian border, had received 2.2 mm of rain between 2130 UTC and 2300 UTC, increasing to 10 mm by 0100 UTC 2 April. Temperature soundings taken from Eucla at 1100 UTC and 2300 UTC 1 April, given in Fig. 2, showed that in the 12-hour period the sub-cloud layer saturated, with the cloud base lowering from an initial height of 17000 ft at 1100 UTC down to the lowest few thousand feet by 2300 UTC. Surface observations of

Fig. 2 Temperature soundings taken from Eucla at 1100 UTC (blue) and 2300 UTC (red) 1 April 2005. Low-level winds for 2300 UTC.

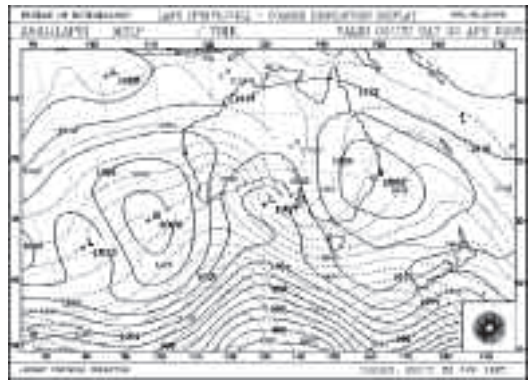


cloud from Eucla at 2300 UTC reported one octa at 1000 ft and four octas at 3000 ft. The rain was mostly confined to west of Nullarbor with no rainfall registered at Nullarbor at this time.

The 1000-500 hPa thickness analysis for 1200 UTC 1 April showed a 578 dm thickness ridge over central Australia with the axis roughly aligned with the western side of Eyre Peninsula. By 0000 UTC this thickness pattern had not changed significantly with the ridge only slightly weaker at 577 dm and aligned over central Eyre Peninsula, as shown in Fig. 3. This suggested that the pre-frontal trough had formed initially on the western side of a 1000-500 hPa thickness ridge under an area of maximum warm air advection responsible for a decrease in density and lowering of pressure.

By 0225 UTC satellite imagery indicated that the middle-level cloud had mostly cleared from over Eyre Peninsula with the main cloudband just west of Ceduna. There was now a pre-existing trough situated to the west of Ceduna, most likely positioned with the leading edge of the cloudband, a dry, hot northerly airstream to the east of the trough and an area of rain or virga to the west of the trough. By 0300 UTC Ceduna had reached its maximum temperature of 38.9°C. It was also at this time that the rain began to reach the ground at Nullarbor, with 1.4 mm recorded between 0300 and 0343 UTC, enhancing the thermal and pressure contrast across the trough boundary such that the temperature difference between the two locations at 0300 UTC was 19°C with a pressure difference of 7 hPa. The trough now represented the boundary between two distinct air masses and the arrival of the trough at Ceduna was marked by the turning of the winds to the southwest with gusts to 18.5 m s⁻¹ at 0319 UTC and a subsequent gust of 20 m s⁻¹ at 0422 UTC.

Fig. 3 1000-500 hPa Thickness analysis (dashed line) 0000 UTC 2 April 2005.



Between 2200 UTC and 2300 UTC when the trough moved through Nullarbor, and 0319 UTC when it reached Ceduna, significant change occurred in the structure of the trough such that it took on the characteristics of a density current and advanced eastward at a speed greater than it had during the morning. Its estimated speed was 14 to 17 m s⁻¹ between Nullarbor and Ceduna, allowing for the uncertainty of the timing of the trough through Nullarbor, increasing to 17 to 19 m s⁻¹ as it moved across Eyre Peninsula. The density current then continued eastwards across central and eastern parts of the State during the afternoon and evening. The density current's foremost point was aligned roughly along latitude 34°S (near the latitude of Adelaide, see Fig. 4), where it was observed to move at a maximum rate of 21 to 22 m s⁻¹.

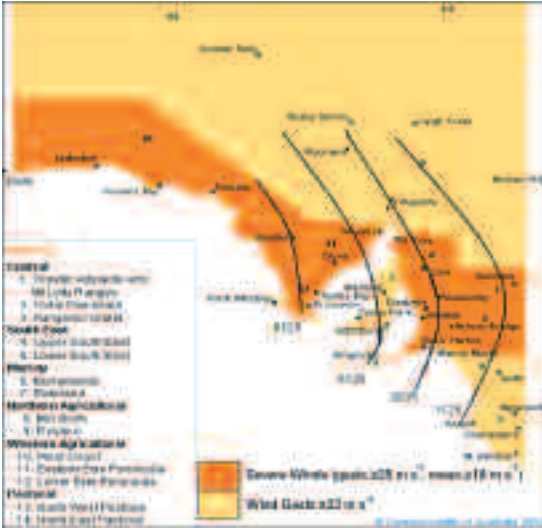
Statewide observations

Surface winds

Fresh and gusty northerly winds turned northwesterly and increased to 10 to 15 m s⁻¹ ahead of the trough before shifting west-southwesterly. Winds remained above 13 m s⁻¹, the strong wind threshold, for typically half to one hour following the wind shift, with several sites recording severe wind gusts, defined as gusts of 25 m s⁻¹ or more, with the passage of the trough.

The position of the trough as it moved across South Australia is shown in Fig. 4. Districts that contained at least one site that recorded severe winds are in dark orange, while districts with sites that recorded

Fig. 4 Passage of the trough as it moved across South Australia, 0525 UTC – 1125 UTC 2 April 2005.



gusts of 22 m s^{-1} or more, a lower threshold of significance to the aviation industry, are shown in light orange. The only district not to meet this lower criterion was Kangaroo Island where the highest gust recorded was 21 m s^{-1} . Significant winds were record-

ed from sites right across the State indicating the widespread nature of the event, with the time between the first and last recorded severe wind gust spanning seven hours.

The strongest gusts measured with the passage of the trough were 29 m s^{-1} at Cleve on Eastern Eyre Peninsula at 0645 UTC and 27 m s^{-1} at Roseworthy in the Mid North at 0920 UTC. Gale force mean winds (18 m s^{-1} or more) were measured at Port Lincoln on Lower Eyre Peninsula for over an hour from 0700 UTC. The maximum wind gusts are shown in Table 1.

Upper winds

Winds below 30 000 ft were available from balloon flights taken from Ceduna Meteorological Information Office (MIO) and Adelaide Airport Meteorological Office ahead of and following the trough, as shown in Table 2. North to northwesterly winds extended throughout the levels ahead of the trough but were observed to strengthen and turn southwesterly to a depth of 5000 ft following the trough. The 0500 UTC wind flight at Ceduna, taken roughly 1.5 hours after the arrival of the trough, showed a 2000 ft wind from the southwest (235 degrees) of 29 m s^{-1} . The 2000 ft wind at Adelaide, also roughly 1.5 hours following the change but six hours following the change through Ceduna, was southwest (235 degrees) at 24 m s^{-1} , highlighting the strength and longevity of the change and the potential for significant or severe gusts at the ground.

Table 1. Maximum wind gusts $\geq 22 \text{ m s}^{-1}$, South Australia, 2 April 2005. (Gusts $\geq 25 \text{ m s}^{-1}$ are shown in bold.)

Site	District	Time (UTC)	Wind direction	Gust (m s^{-1})
Wudinna	West Coast	0551	270	26
Cleve	Eastern Eyre Peninsula	0645	260	29
Cooper Pedy	Northwest Pastoral	0724	230	23
Warburto Point	Yorke Peninsula	0753	320	23
Port Lincoln	Lower Eyre Peninsula	0800	260	23
Snowtown	Mid North	0856	260	26
Whyalla	Eastern Eyre Peninsula	0900	230	22
Port Augusta	Flinders	0901	230	23
Outer Harbour	Adelaide/Mt Lofty Ranges	0913	250	25
Roseworthy	Adelaide/Mt Lofty Ranges	0920	310	27
Parafield	Adelaide/Mt Lofty Ranges	0922	320	25
Edinburgh	Adelaide/Mt Lofty Ranges	0933	270	24
Mount Crawford	Adelaide/Mt Lofty Ranges	0947	260	23
Mount Lofty	Adelaide/Mt Lofty Ranges	0952	220	24
Edithburgh	Yorke Peninsula	0956	260	22
Sellicks Hill	Adelaide/Mt Lofty Ranges	1000	250	24
Oodnadatta	Northeast Pastoral	1007	210	22
Renmark	Riverland	1204	350	25
Lameroo	Murraylands	1220	280	26
Mount Gambier	Lower SE	1256	320	22
Naracoorte	Upper SE	1301	250	22

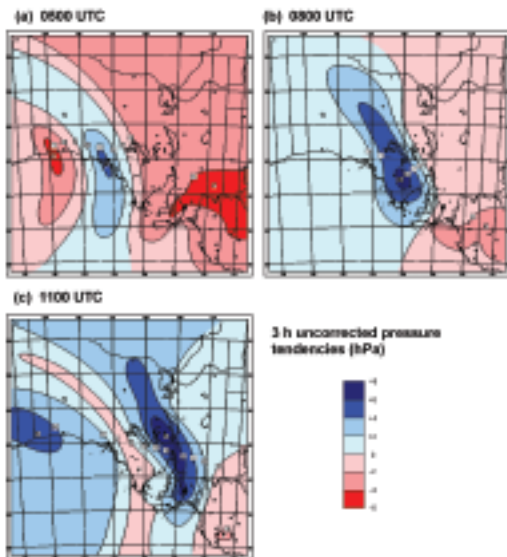
Table 2. Upper-level winds ahead of and following the trough at Ceduna at 2300 UTC 1 April 2005 and 0500 UTC 2 April 2005 and Adelaide Airport at 0500 UTC and 1100 UTC 2 April 2005. Height based on pressure levels, approximate only.

Height (ft)	<i>Ahead of the trough</i>				<i>Following the trough</i>			
	<i>Ceduna 2300 UTC</i>		<i>Adelaide 0500 UTC</i>		<i>Ceduna 0500 UTC</i>		<i>Adelaide 1100 UTC</i>	
	<i>Wind direction</i>	<i>Speed (m s⁻¹)</i>	<i>Wind direction</i>	<i>Speed (m s⁻¹)</i>	<i>Wind direction</i>	<i>Speed (m s⁻¹)</i>	<i>Wind direction</i>	<i>Speed (m s⁻¹)</i>
30000	325	35	305	42	325	54	310	53
23500	315	32	320	28	320	40	320	42
18500	330	10	330	21	330	30	330	33
14000	310	11	330	15	350	26	335	22
10000	305	19	335	16	340	19	325	19
5000	345	15	350	13	275	11	255	25
2000	360	22	330	13	235	29	235	24
0	010	11	315	8	230	14	215	7

Pressure

The three-hour uncorrected pressure tendencies for 0500 UTC, 0800 UTC and 1100 UTC 2 April 2005 are shown in Fig. 5. The surface pressure fell ahead of the trough, enhanced by the mostly clear and hot conditions during the afternoon with the greatest falls of 4 hPa over three hours observed at 0500 UTC. Following the trough the cooler, denser air resulted in the pressure rising markedly, with three-hour tendencies of +4 hPa at 0500 UTC increasing to +6 hPa by 0800 UTC and 1100 UTC.

Fig. 5 Three-hour uncorrected pressure tendencies at (a) 0500 UTC, (b) 0800 UTC and (c) 1100 UTC, South Australia, 2 April 2005. Charts provided by Bob Schahinger, South Australian Regional Office.



Visibility in dust

Dust was observed, or inferred, at a number of sites from satellite imagery, ceilometers, visibility meters and ground reports. The dust occurred in the northerly winds ahead of the trough as well as in the south-westerly winds following the trough, with the latter event being the more significant of the two.

There were numerous indicators of dust in the northerly winds ahead of the trough. Ceilometer data from Port Lincoln Airport suggested the presence of raised dust as early as 0000 UTC, while satellite imagery showed dust, or salt, blowing from Lake Eyre at this time. Observers at Ceduna MIO and Woomera MIO reported raised dust at 0230 UTC, with reductions in visibility to 8 km reported at Adelaide Airport at 0700 UTC and similar conditions indicated by the visibility meter at Edinburgh RAAF Base, 25 km north of Adelaide.

However, the significant visibility reductions came with the arrival of the density current at the trough's leading edge. Infrared satellite imagery from GOES-9 in Fig. 6 shows the discrete edge of the dust bounded by the density current, marked as the discontinuity between the hot, dry air ahead of the trough and the cooler air following the trough. The onset of dust was coincident with the arrival of the cooler air, with clearance times of the dust and rate of movement of the trough suggesting that the dust extended westward to the middle-level cloud-band visible on the satellite imagery, approximately 160 km to the west.

The arrival of the dust (Fig. 7) brought a sudden and sharp decrease in visibility, with the visibility typically remaining below pre-trough levels for more than one and half hours following passage of the trough. The greatest reduction in visibility was observed during the initial onset of the dust with reports as low as 577 m at Edinburgh, 1000 m at Whyalla and 3500 m at Ceduna and Woomera.

Fig. 6 GOES-9 Infrared Satellite Imagery over South Australia showing dust bounded by the density current at the trough's leading edge at (a) 0825 UTC and (b) 0925 UTC 2 April 2005.

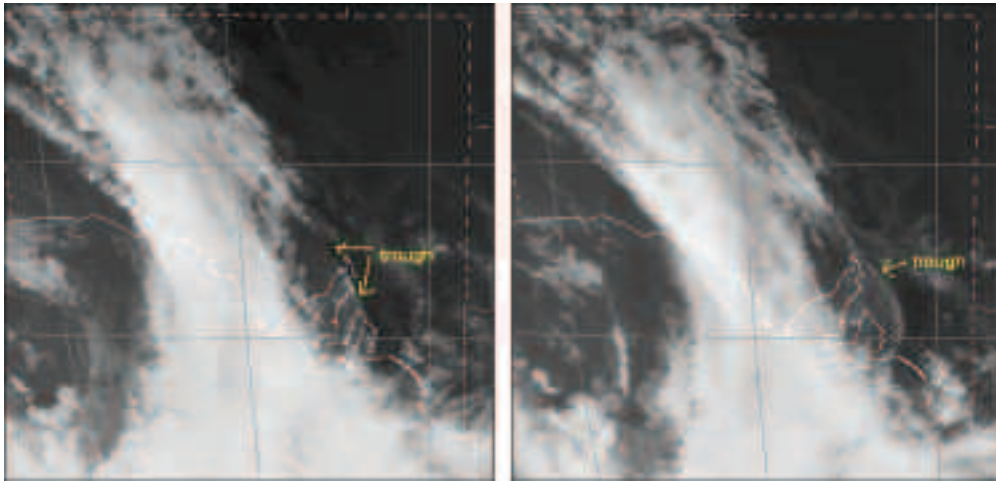


Fig. 7 Dust trapped within the density current extending over Lucky Bay, South Australia, 2 April 2005. Photo courtesy Donna Lamb, Cowell, with Jamie Docking and his dog Indy pictured. Photo previously published in the *Eyre Peninsula Tribune*, 7 April 2005. Inset: Location of Lucky Bay on Eyre Peninsula, SA.



Temperature and humidity

Many sites across South Australia experienced record high April maximum temperatures in the northerly airstream, with maxima ahead of the trough ranging from the low to mid 30s in the southeast to more than 40°C over Eyre Peninsula and the north of the State. Southwest winds following the trough brought a marked cooling, with sites that were near their maximum temperature at the time of the wind change observing falls in temperature of around 10°C over a

period of one hour. The thermal contrast across the trough boundary is highlighted in Fig. 8 which shows air temperature at 0500 UTC. At this time the trough was moving across western Eyre Peninsula where the temperature gradient following the trough was approximately 1.5°C per 10 km.

Charts of maximum temperature across South Australia for 2 April 2005 and the departure from the mean conditions are given in Fig. 9. The early arrival time of the trough in the west, with it having reached

Fig. 8 Air temperature, South Australia, 0500 UTC 2 April 2005. Chart provided by Bob Schahinger, South Australian Regional Office.

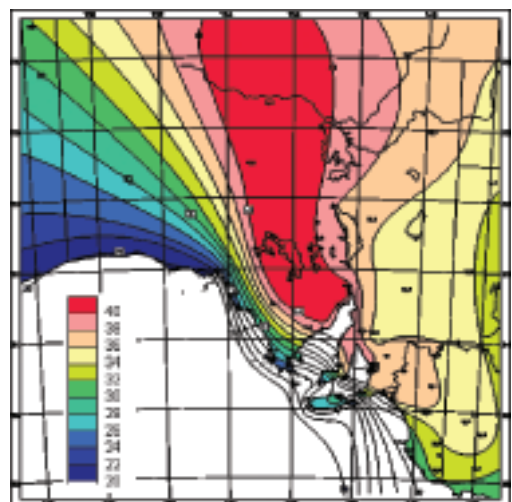
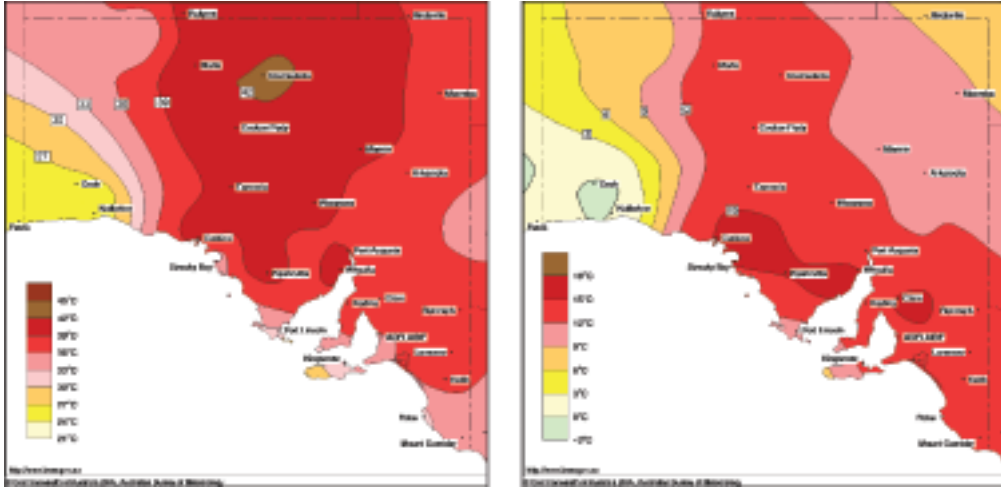


Fig. 9 (a) Maximum temperature and (b) maximum temperature anomaly, South Australia, 2 April 2005. Charts provided by Robert Nash, National Climate Centre.



Nullarbor by 2300 UTC 1 April, is reflected in the lower maximum temperatures obtained in the area. Further east, temperatures were typically 12 to 15 degrees above the 2 April average.

Humidity increased across the trough boundary with rising dew-points and falling temperatures. Dew-point temperatures were typically 10°C in the northerly winds well ahead of the trough but approached 5°C just ahead of the wind change with some northern sites measuring below zero. Dew-points were then observed to jump to around 15°C immediately following the trough, resulting in a rise in relative humidity from initial values of 15 to 20 per cent to around 50 per cent following the trough.

Examination of the density current at Edinburgh RAAF Base

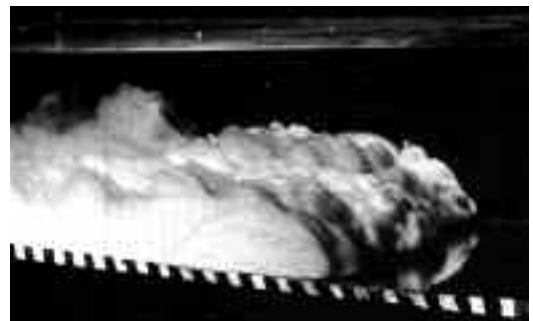
Density currents are established when a colder, denser air mass enters into and displaces a pre-existing environment of lower density. Common examples of density currents include cold fronts, thunderstorm outflows and sea-breezes.

Density currents move at a speed dependent on the unique characteristics of the density current, including the height to which it extends, the ambient air and the surface over which it travels. They can produce significant turbulence at the interface between the two air masses with significant mixing of the air within

the density current. Studies of density currents, such as laboratory investigations by Simpson and Britter (1980), and observational studies including work by Sun et al. (2002) that focused on the intermittent turbulence associated with the passage of a density current, have revealed much about their characteristics and behaviour. An image of a density current generated in the laboratory by releasing a denser fluid into a lighter fluid in a glass tank is shown in Fig. 10.

On 2 April 2005 the effect of a pre-frontal trough with a hot northerly airstream to the east and a precipitating cloudband to the west was to produce a density current that advanced eastward ahead of the

Fig. 10 A density current in a glass tank. Photo by J.E. Simpson, University of Cambridge.



cloudband at a speed greater than that of the pre-existing trough. A detailed analysis of this density current as it moved through Edinburgh RAAF Base, 25 km north of Adelaide, can be made through investigation of the one-minute data available from the site for pressure, wind speed and direction, temperature, dew-point and visibility. The density current onset time was given as 0917 UTC, immediately before the greatest rate of change in pressure.

Time series of visibility, pressure, temperature and dew-point, wind direction and wind gusts for the period 0500 – 1400 UTC are given in Figs 11(a) – (e). These time series clearly show the change of environment at Edinburgh as the density current moved across the site. In this section the height and propagation speed of the density current are calculated, with consideration given to the processes involved in the generation of the initial wind gust. Special attention is returned to the pressure, wind speed and visibility later in the section with a periodic variation revealed in the data within the first half hour of the passage of the density current, varying according to the Brunt-Väisälä frequency. This is attributed to the existence of internal gravity waves at the head of the density current.

Pressure

Figure 11(a) indicates that the pressure at Edinburgh fell only weakly during the afternoon, from 1004.5 hPa at 0500 UTC to just below 1003 hPa before the density current arrived at 0917 UTC. The density current then brought a rapid change in pressure, which rose by 1.3 hPa in the first two minutes after the initial onset and then continued to rise at a relatively uniform rate over the next 90 minutes to 1009.4 hPa at 1045 UTC. The pressure peaked at 1010.2 hPa, 45 minutes later, resulting in an overall rise of 7.3 hPa in 2.2 hours, before it started to gently fall again.

Temperature and dew-point

Time series of the temperature and dew-point at Edinburgh RAAF Base are given in Fig. 11(b). During the afternoon the temperature was in the high 30s with a maximum of 39.3°C observed at 0615 UTC, before gradually falling in the early evening to around 34°C ahead of the density current. The temperature then fell rapidly, again with the greatest change observed in the first few minutes following the density current, dropping to 31°C by 0920 UTC, just three minutes after onset. After this initial discontinuity the temperature then continued to fall logarithmically throughout the evening, as shown in Fig. 12, such that the temperature T_t at time t after the arrival of the density current could be represented by an equation of the form

$$T_t = T_o - \alpha \ln(t) \quad \dots 1$$

where T_o is the initial temperature and $\alpha = \text{constant}$, so that within half an hour the temperature had dropped by five degrees to 26°C, lowering to 24°C over the subsequent 90-minute period.

The dew-point meanwhile had been steady near 10°C during the late afternoon but jumped suddenly by three degrees at 0919 UTC, two minutes after the density current's arrival. The dew-point then continued to climb to 16°C in the next fifteen minutes before settling to around 15.5°C for the rest of the evening.

Wind

Figure 11(c) shows the wind direction before and after the passage of the density current. Ahead of the density current winds remained in the northerly sector, turning through the northwest to west in the first few minutes following the density current and only maintaining a southwesterly direction after 15 minutes. The strength of the wind gusts increased markedly with the onset of the density current, as shown in Fig. 11(d), with gusts to 22 m s⁻¹ within the first four minutes and reaching a maximum of 24 m s⁻¹ at 0933 UTC.

Visibility

The visibility at Edinburgh RAAF Base plummeted with the onset of the density current and associated dust as shown in Fig. 11(e). Within five minutes of the arrival of the density current the visibility had dropped to its lowest value of 577 m and remained below 4000 m for three-quarters of an hour. The visibility gradually improved over the following hour to conditions similar to those ahead of the density current as the wind moderated.

Height of the density current

The height of the density current is determined by assuming that the changes in pressure are a direct result of the intrusion of the colder, denser air. Following Garratt (1984) it is further assumed that the two air masses are well mixed and that the pressure changes occur under a state of hydrostatic balance. Therefore, by employing the hydrostatic and gas equations

$$\frac{\partial p}{\partial z} = -\rho g \quad \dots 2$$

and

$$p = \rho RT \quad \dots 3$$

and integrating Eqn 2 over height h and differentiating with respect to time it can be shown that the change in pressure, Δp , can be approximated by

Fig. 11 Time series of (a) pressure, (b) temperature and dew-point, (c) wind direction, (d) wind gusts and (e) visibility from one-minute data, Edinburgh RAAF Base, 2 April 2005. Density current arrival time 0917 UTC (dashed line).

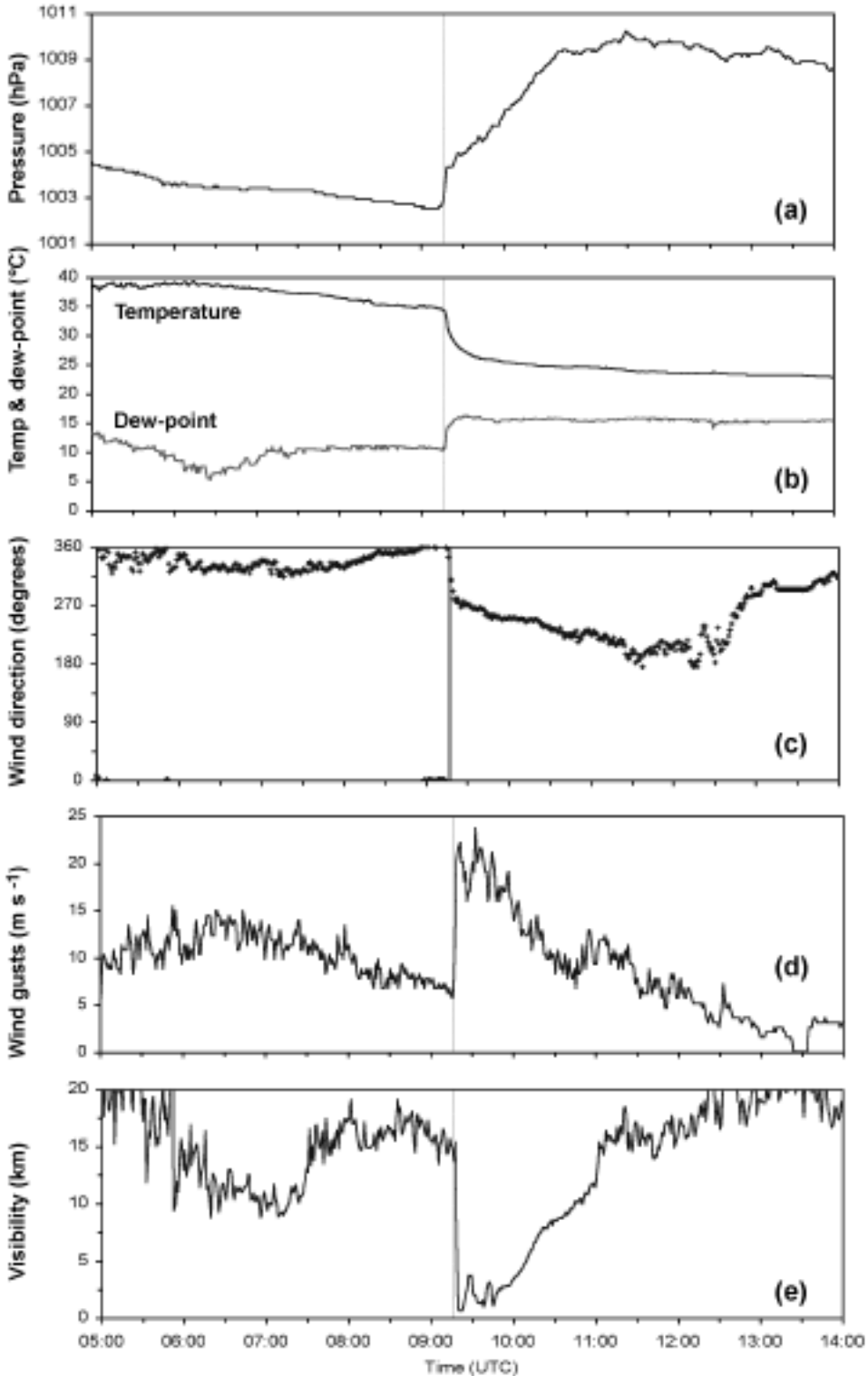
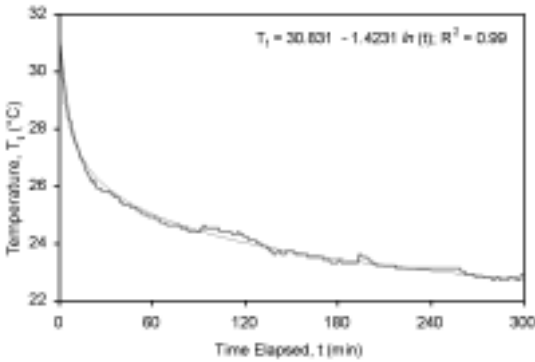


Fig. 12 Logarithmic decay in temperature following the passage of a density current at Edinburgh RAAF Base 2 April 2005. Elapsed time commencing 0920 UTC. $T_t = 30.831 - 1.4231 \ln(t)$; where temperature T_t is in degrees Celsius and time t is in minutes.



$$\Delta p = \frac{ghP}{RT^2} \Delta T \quad \dots 4$$

where ΔT is the temperature difference between the ambient air and the density current, h is the height of the density current, T is the ambient temperature, P is the ambient pressure, g is the acceleration due to gravity and R is the universal gas constant.

The height of the density current can therefore be calculated by simple rearrangement of Eqn 4. The resulting height profile of the density current as it moved through Edinburgh RAAF Base, as constructed from one-minute pressure data, is shown in Fig. 13. At the onset of the density current the ambient temperature was 34.2°C, giving $\Delta T \approx 10^\circ\text{C}$ assuming a mean density current temperature of 24°C, and the ambient pressure was 1002.9 hPa. The density current showed good levelling out at 1045 UTC at a height of ~1760 m (~5780 ft), approximately 1.5 hours after the initial onset. Subsequent changes in pressure and temperature were only small suggesting that this represented the full height of the density current.

Horizontal winds in the lowest few kilometres were available from the Buckland Park wind profiler, situated 17 km northwest of the Edinburgh RAAF Base, as shown in Fig. 14. No data were available below 500 m but the wind near 500 m was observed to turn to the southwest at 0930 UTC, with the southwest winds extending to 1 km by around 1000 UTC and 1.5 km by 1030 UTC. This profile agreed extremely well with the calculated height of the density current. Noticeably, the demarcation between the

Fig. 13 Density current height profile as it moved through Edinburgh RAAF Base. Onset time 0917 UTC 2 April 2005.

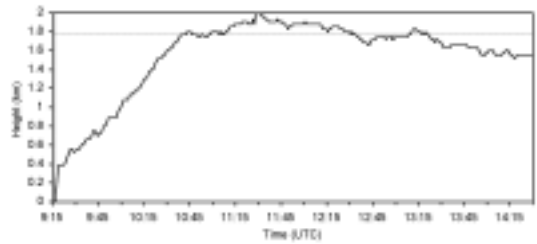
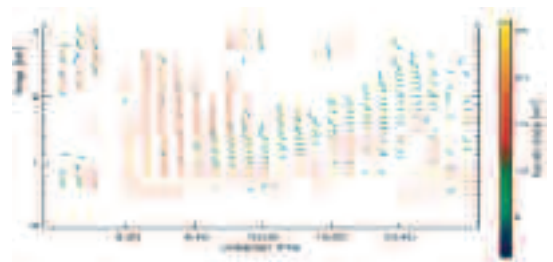


Fig. 14 Horizontal velocity field, Buckland Park 0900 – 1100 UTC 2 April 2005. Wind profile provided by Andrew MacKinnon, University of Adelaide.

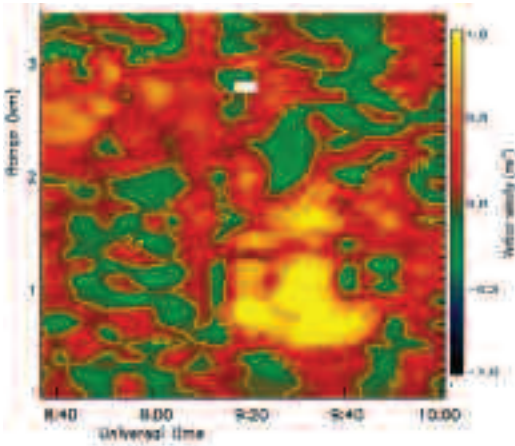


northwest winds aloft and the southwest winds within the density current became less pronounced after 1045 UTC, the time that the density current was shown to level out.

It was observed that the return signal from the profiler was markedly improved with the arrival of the density current. In the well-mixed atmosphere ahead of the density current there would have been little variation in the refractive index along the beam's path resulting in only a weak signal. However, since the refractive index is dependent on temperature and humidity the arrival of the density current created changes in this index which allowed for a greater return signal.

Vertical velocities during this time were also available from Buckland Park as shown in Fig. 15. As with the horizontal wind the data below 500 m were unreliable, but above this level a marked upward (positive) motion was indicated just prior to 0920 UTC, coincident with the arrival of the density current, with a distinct signal to a height of 1 to 2 km that persisted for approximately 30 minutes. With sufficient mois-

Fig. 15 Vertical velocity field, Buckland Park 0900 – 1000 UTC 2 April 2005. Wind profile provided by Andrew MacKinnon, University of Adelaide.



ture it would be expected that a thin layer of cloud would form in this area of up motion. Photographs shown in Fig. 16 of the dust bounded by the density current taken near Whyalla, on Eyre Peninsula, supported this with stratocumulus cloud visible at the density current's leading edge.

Speed of propagation

Theory predicts that the speed at which the density current propagates, c , depends on the relative change in density and on the height to which the density current extends such that

$$c = \sqrt{\frac{\Delta\rho}{\rho} gh} \quad \dots 5$$

where $\Delta\rho$ is the change in density, ρ is the density of the ambient air, g is the acceleration due to gravity and h is the height of the density current.

Equivalently,

$$c = \sqrt{\frac{\Delta p}{\rho}} \quad \dots 6$$

where Δp is the change in pressure.

The density current was observed to level out at 1045 UTC at which time the pressure had risen by 6.5 hPa, which, by using Eqn 6, gives a propagation speed of 24 m s⁻¹. This compares well with the rate of movement determined from radar imagery, which showed the trough as it moved from Edinburgh to the east with an average speed of 21 to 22 m s⁻¹. It is also of interest to note that this exactly matched the highest gust recorded at Edinburgh 15 minutes after the initial onset time.

Fig. 16 Dust trapped within the density current with a thin layer of stratocumulus cloud aloft as the air is forced upwards. Photograph taken at Whyalla, Eyre Peninsula, 2 April 2005, courtesy of Paul Michalak and Renee Hanson, Whyalla. Photo previously published in the *Whyalla News*, 7 April 2005.



Generation of the initial wind gust

Three-hour pressure tendencies are commonly used as a measure of the strength of a wind change associated with the passage of a density current, with strong pressure rises and falls either side of the change indicating the likelihood of significant wind gusts arising from the isallobaric component of the wind speed.

However, if the pressure changes are calculated over a much shorter time interval, for example over two minutes, the pressure is seen to spike with the arrival of the density current with insignificant changes in pressure after that time. Figure 17 shows the pressure tendencies at Edinburgh RAAF Base on 2 April 2005 between 0600 and 1400 UTC measured at two-minute and three-hourly intervals. The two-minute data is seen to rise by 1.3 hPa in the first two minutes following the density current, while the three-hour tendencies peaked much later with the arrival of the density current actually marking the change from negative to positive tendencies.

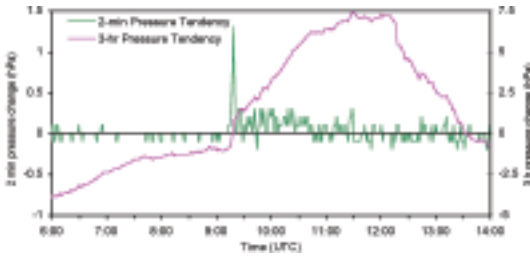
This sudden increase in pressure with the arrival of the density current would produce a local change in momentum and hence a change in wind speed.

From Newton's Second Law of Motion,

$$\frac{\partial V}{\partial t} = -\rho^{-1} \nabla p \quad \dots 7$$

Given that the density current was travelling towards the east, the pressure gradient was directed along the x-axis simplifying Eqn 7 to the form $\partial u/\partial t = -\rho^{-1} \partial p/\partial x$.

Fig. 17 Two-minute and three-hour uncorrected pressure tendencies, Edinburgh RAAF Base, 2 April 2005.



Over the two-minute period of greatest pressure rise and under the assumption of a steady-state propagating system, the horizontal pressure gradient can be approximated by

$$\frac{\partial p}{\partial x} = \frac{-1}{c} \frac{\partial p}{\partial t} \quad \dots 8$$

Returning to the simplified form of Eqn 7 the change in wind speed, Δu , can therefore be approximated by

$$\Delta u = \frac{-1}{\rho c} \frac{\partial p}{\partial t} \Delta t \quad \dots 9$$

Over the two-minute period $dp/dt = 0.65$ hPa min⁻¹, the mean temperature and pressure were 33.6°C and 1003.5 hPa respectively, giving $\rho = 1.140$ kgm⁻³, and with $c = 22$ m s⁻¹, then the change in wind speed, $\Delta u = 5.2$ m s⁻¹ from the west.

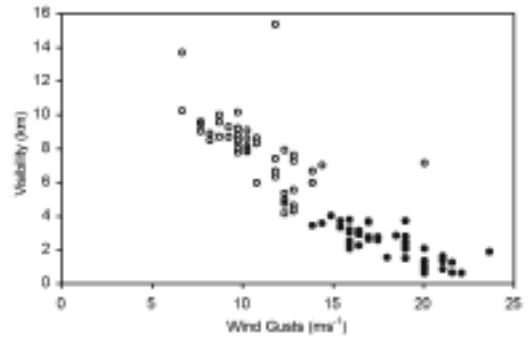
With an initial wind speed of 6.2 m s⁻¹ from 343 degrees (NNW) this gives a resultant wind of 9.2 m s⁻¹ from 310 degrees (NW).

The actual wind was observed to increase to 17 m s⁻¹ from 308 degrees by this time, so while the backing of the wind was well represented the speed was underestimated. Garratt (1984) carried out a similar analysis for a pressure jump line and he also found that the increase in speed was underestimated. However, as he remarked, in such calculations no consideration is given to the turbulent nature of the wind.

Periodicity of the wind, visibility and pressure

A close correlation existed between the strength of the wind and the visibility following the density current such that the greatest reductions in visibility coincided with the strongest wind gusts. This is highlighted in Fig. 18 where visibility is plotted as a function of wind gusts for the initial 90-minute period following the density current. The time series of visibility shown in Fig. 11(e) showed that the visibility was consistently below 4 km between 0920 and 1005 UTC during which time the wind gusts did not ease

Fig. 18 Visibility vs wind gusts at Edinburgh RAAF Base during the 90 minutes following a density current, commencing 0917 UTC 2 April 2005. ● – visibility consistently below 4 km between 0920 and 1005 UTC.



below 13 m s⁻¹, with gusts of 20 m s⁻¹ reducing the visibility further to 2 km and below.

In addition to the inverse relationship between the wind and visibility, both were observed to vary periodically during the initial half hour following the density current, as highlighted in Fig. 19(a), and their values could be approximated by the expressions

$$\text{Wind speed} = 16.7 + 2.9\cos(Nt) \text{ m s}^{-1} \quad \dots 10$$

$$\text{Visibility} = 2.2 + 1.6\cos(Nt - \pi) \text{ km} \quad \dots 11$$

N is the Brunt-Väisälä frequency, or buoyancy frequency, such that

$$N^2 = \frac{g}{\theta} \frac{\partial \theta}{\partial z} \quad \dots 12$$

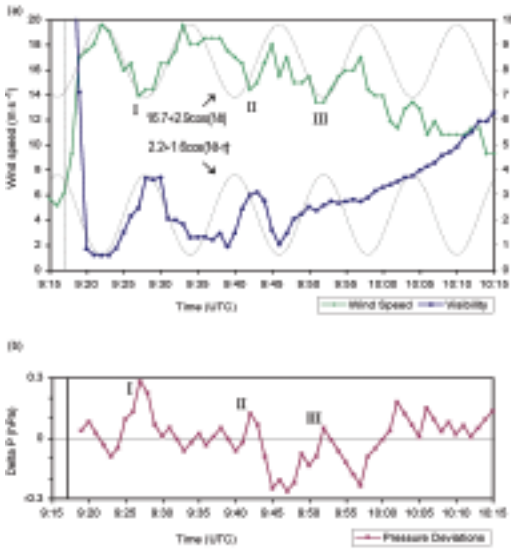
where θ is potential temperature and g is the acceleration due to gravity.

The Brunt-Väisälä frequency relates to the oscillations a particle will experience if displaced from an initial position of vertical equilibrium, and arises due to the stratification of the atmosphere, in this case, at the head of the density current. Such oscillations set up internal gravity waves whose period, T' , is dependent on N such that $T' = 2\pi/N$.

From the observed wind and visibility data the period was found to be 12 minutes giving a value of $N = 8.73 \times 10^{-3} \text{ s}^{-1}$. The best fit to the data occurred within the first one and a half cycles, completed by 0935 UTC.

Lack of upper air temperature and pressure data at the time of the passage of the density current makes this value difficult to verify. There were, however, data available from a balloon flight taken from Adelaide Airport at 1100 UTC, approximately 90 minutes after the passage of the density current.

Fig. 19 (a) Sinusoidal variation in one-minute mean wind speed and visibility and (b) deviations in pressure, ΔP , from the mean rising trend following the passage of a density current, Edinburgh RAAF Base, 2 April 2005. The local minima in wind speed and maxima in pressure coincide at points I, II and III.



It was considered that the temperature and pressure data from the radiosonde taken from below the height to which the density current extended at the time that the oscillations were observed would be reasonably representative of the environment that existed within the density current. At 0935 UTC, the time chosen because of the good fit with the cosine relationship and the completion of exactly one and a half cycles, the density current extended to a height of 607 m. Therefore a combination of surface data from Edinburgh and data near 607 m above the surface from Adelaide Airport at 1100 UTC was used to construct an approximate vertical profile of the density current as it moved through Edinburgh some 90 minutes earlier, allowing for the calculation of the Brunt-Väisälä frequency. The potential temperature, θ , and

height, z , are given by

$$\theta = T (p_o/p)^{\frac{R}{C_p}} \quad \dots 13$$

where $p_o = 1000$ hPa, $R = 287$ Jkg⁻¹K⁻¹, $C_p = 1000$ Jkg⁻¹K⁻¹

and
$$z = R\bar{T}/g \ln(p_2/p_1) \quad \dots 14$$

where \bar{T} = mean layer temperature, respectively. The values used are given in Table 3, giving $N = 8.90 \times 10^{-3}$ s⁻¹ and $T' = 11.8$ min, which is in excellent agreement with the observed values.

The relationship between the fluctuation in wind speed and pressure was also considered. As already demonstrated in Fig. 11(a), after an initial jump of 1.3 hPa in the first two minutes following the density current, the pressure showed a mean rising trend. The gradient of the rising pressure was calculated for the period 0919 UTC, after the initial jump, through to 1015 UTC, and the deviation from this trend was plotted in Fig. 19(b). The pressure was observed to vary between ± 0.3 hPa of the mean rising trend. Comparing the deviations in pressure with the fluctuations in wind speed, it was observed that the local pressure rises corresponded exactly with the local minima in wind speed, marked as I, II and III in Fig. 19.

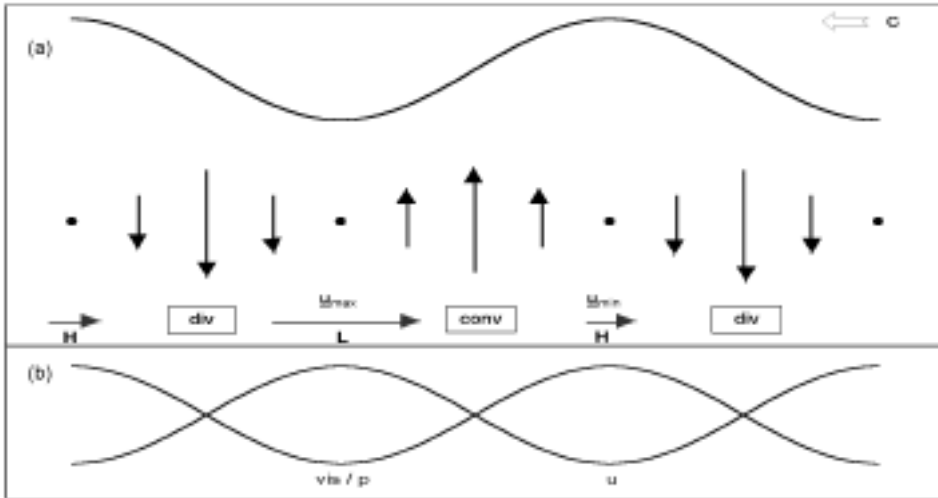
Generation of internal gravity waves at the density current head

The observed oscillations in wind speed, visibility and pressure, and the relationship between the three elements, indicated the presence of internal gravity waves generated at the head of the density current, opposing the flow of the surface wind. A schematic of the gravity wave is shown in Fig. 20. The gravity wave is shown propagating to the left with the surface wind to the right. For such a wave the resultant vertical velocities and horizontal surface winds would have been as shown: convergence and rising air ahead of the local low pressure and divergence and descending air ahead of the high. As a consequence the greatest wind speed would coincide with the lowest pressure and the lowest wind speed with the greatest pres-

Table 3. Calculation of the Brunt-Väisälä frequency, N , based on surface data from Edinburgh RAAF Base and upper air data from Adelaide Airport 1100 UTC 2 April 2005.

Location	Pressure (hPa)	Temp (°C)	Potential Temp (°C)	Height (m)	N (10^{-3} s ⁻¹)	T' (min)
Edinburgh	1009.4	24.5	23.7	0	8.90	11.8
Adelaide	941	20	25.2	607.0		

Fig. 20 (a) Schematic of the gravity wave. Direction of propagation of wave, c . Time of greatest/least wind speed (u_{\max}/u_{\min}) corresponding with minimum/maximum pressure (L/H). Convergence/divergence ahead of/following the low pressure and associated vertical motion indicated by vertical arrows. Increased/decreased visibility corresponding with upward/downward vertical motion. (b) Phase relationship between visibility (vis), pressure (p) and wind speed (u).



sure. These results are consistent with studies of internal gravity waves by Eom (1975) and Kusunoki and Eito (2003) who also found a half-cycle phase difference between pressure and wind speed perturbations.

The visibility on the other hand, which was dependent on the concentration of the dust within the density current, was shown to be in phase with the pressure. Under the area of high pressure, the density current would have shown a local peak in height, mixing the dust over the greatest depth and lowering the concentration and, in turn, increasing the visibility. Conversely, the visibility was at its lowest under the low pressure, where the dust would have been mixed over the least depth. The phase relationship between the visibility, pressure and wind speed is shown in Fig. 20(b).

Returning to the time series in Fig. 19, by 1005 UTC the visibility had risen to 4 km and the wind had eased below 13 m s^{-1} with neither element showing any periodic variation. Typically, gravity waves will only last for about one wavelength in the absence of a trapping mechanism, as discussed by Crook (1988). Beyond this time the energy of the wave would have dissipated.

Antecedent weather conditions

There were several important precursors to the dust event, most notably the dry lead-up conditions and the

local contribution over Lower Eyre Peninsula from the bushfire that occurred during January 2005.

Rainfall

In the preceding three months rainfall across South Australia had been mostly average to below average with parts of Eyre Peninsula and the far north of the State having received very much below average rainfall.

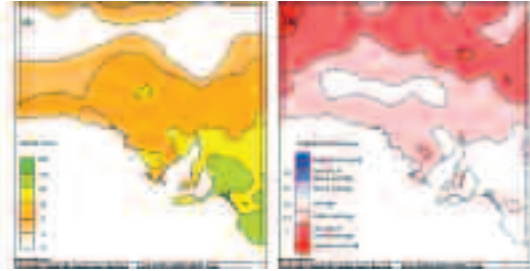
The rainfall totals for South Australia for the period 1 January to 31 March 2005 and the rainfall deciles for the same period are shown in Fig. 21. No additional rainfall was recorded from across the State on 1 April 2005.

Crop and pasture reports from the Department of Primary Industry and Resources, SA (DPIR 2005) indicated that the dry conditions had resulted in generally no sub-soil moisture across Eyre Peninsula and that due to the poor crop season the previous year there were many bare paddocks across central and eastern Eyre Peninsula vulnerable to wind erosion.

Lower Eyre Peninsula fire

On 11 January 2005 a devastating fire spread from Wangary, on Lower Eyre Peninsula, to the east and northeast, burning an estimated area of 83000 ha. Stubble paddocks were burnt to the ground with the topsoil quickly eroding, exposing the sandy undersoil, while through forest the intense burning produced extensive areas of fine white ash. These fires signifi-

Fig. 21 South Australian rainfall (a) totals and (b) deciles for the three-month period 1 January to 31 March 2005, National Climate Centre. No additional rainfall was recorded on 1 April 2005.



cantly increased the amount of debris available in the local area to be raised as blowing dust. Photographs of a bare paddock and burnt forest taken from the area just a few days after the fire are shown in Fig. 22.

Impact across South Australia

The impact of the dust and severe wind event were widely felt across South Australia. Strong winds and poor visibility associated with the dust produced hazardous driving conditions with reports of highway traffic slowed to 30 km/h in the State's Mid North. Emergency services were called to four road accidents, with two people taken to hospital for minor injuries after one of the accidents. Strong winds uprooted large trees on a property in the Mid North, bringing down power lines and cutting electricity. Damage to a shed and annex was reported in

Adelaide, while fences were brought down and fallen trees blocked roads across many parts of the State including Eyre Peninsula and the South East. Severe winds were recorded in seven of the fourteen forecast districts, indicating the widespread nature of the event and the potential for damage over a considerable area of the State. Across the metropolitan area along the State Emergency Service responded to 41 calls for assistance in the two-hour period following the event.

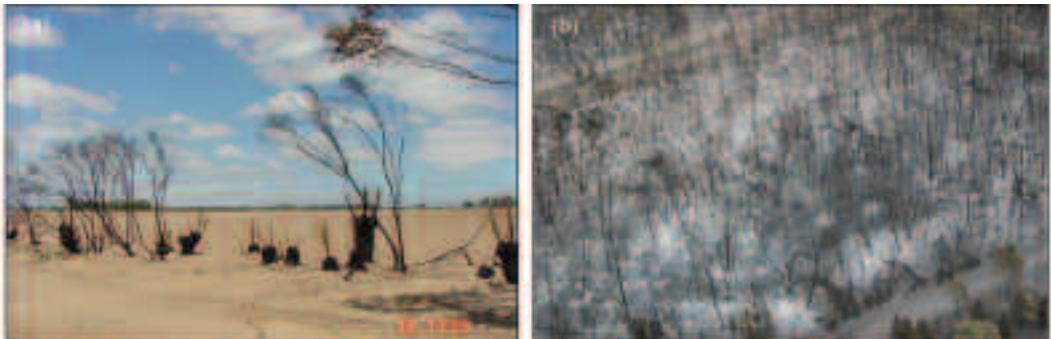
Industry concerns

Visibility reductions and the strong winds were a concern to both the aviation and marine industries with timely and accurate forecasts of the essence, with many warning criteria met.

Aviation. (a) Visibility was reduced to below alternate conditions, the minimum level at which aircraft must carry extra fuel to allow for a diversion, at a number of airports for periods of around an hour. (b) The vertical and horizontal extent of the dust presented a potential hazard to aircraft in flight. (c) Wind gusts in excess of 22 m s^{-1} were observed at a number of airports, gusts considered strong enough to adversely affect aircraft on the ground. (d) The strength of the low-level winds in the northwest to southwest flow would have been likely to result in mechanical turbulence, with the potential for mountain waves and severe turbulence in the lee of the Mount Lofty Ranges to the east of Adelaide.

Marine. Widely observed mean winds of 13 m s^{-1} and above warranted the issue of Strong Wind Warnings over affected coastal waters with the additional requirement of localised gale force wind squalls due to the longevity and severity of the wind gusts.

Fig. 22 Photos following the Lower Eyre Peninsula fires January 2005 showing (a) burnt stubble paddock with sandy undersoil exposed and (b) white ash. Photos courtesy Kirsty Turner, Bureau of Meteorology Training Centre and the Bushfire Cooperative Research Centre.



Severe weather. Gusts of 25 m s^{-1} or more were measured at eight sites across South Australia with mean winds of 18 m s^{-1} recorded at Port Lincoln on Lower Eyre Peninsula. These observations met the criteria for Severe Weather Warnings across seven of the State's fourteen forecast districts.

Numerical weather prediction

The 5 km grid resolution MESOLAPS computer model was run over the South Australian domain for the 24-hour period commencing 1200 UTC April 1 2005. The model identified the pre-frontal trough as a west to southwest wind change roughly aligned with a middle-level cloudband. The model placed the wind change near Ceduna at 0400 UTC, moving east to cross the west coast of the Eyre Peninsula between 0500 UTC and 0600 UTC, which agreed well with the observed wind change in the area. The model accurately depicted the position of the middle-level cloud and associated rainfall at this time, advancing the cloud and rain-bands eastward during the day at a rate comparable with observations. However, the predicted wind change subsequently slowed in comparison to its actual movement such that it only reached the Adelaide area by 1100 UTC, around 90 minutes after the observed wind change and by which time it had moved inland to the Riverland and eastern districts of South Australia.

Pre-frontal trough temperatures from the model were generally underestimated, with discrepancies of typically two to five degrees, however on a day of record-high maxima this was to be expected. However, of greater significance was the fact that the model did not identify the sharp fall in temperature following the wind change. Across Eyre and Yorke Peninsulas model output temperatures remained in the high 20s into the evening several hours following the change, compared with observed temperatures falling to near 20 degrees.

Upper winds obtained from balloon flights taken over Adelaide Airport before and after the passage of the trough, given in Table 2, were compared with the MESOLAPS output. Ahead of the trough the wind profile was reasonably well represented, although underestimated by about 5 m s^{-1} from the surface to 300 hPa. Both modelled and observed winds increased following the trough although the model again underestimated the winds. Above 6000 ft the discrepancy was generally no more than the 5 m s^{-1} observed ahead of the trough however the structure and strength of the winds in the lowest few thousand feet was not well simulated. Observations showed that the southwest winds following the trough extended to a height of 6000 ft with winds of 20 to 25 m s^{-1} , while the model only had southwest winds to 3000 ft with strengths typically 10 to 15 m s^{-1} less than this.

The 5 km grid resolution MESOLAPS was therefore shown to have identified the pre-frontal trough and trailing cloud and rain-band with a high degree of accuracy, however, the thermal contrast across the trough boundary was not well recognised and it was unable to simulate the development of the density current that ensued. As such the eastward advancement of the wind change, the strength of the winds and the depth over which the change extended were subsequently underestimated.

Future directions

This case study highlighted the complexity of pre-frontal trough systems with the possible development of density currents and severe weather. The dry lead-up conditions contributed to the available dust that produced significant reductions in visibility, with the wind speed and dust concentrations further complicated by the existence of internal gravity waves at the head of the density current. A strong correlation was shown between the wind strength and visibility during this event, however further investigation into a range of dust events would be required to develop more generalised rules. The increasing number of observation sites with visibility meters should allow for more in-depth and accurate analyses, with sites that record both one-minute wind and visibility providing the best comparative data. However, any such relationships would be dependent on the location and pre-existing environmental conditions.

Further studies could also include investigation into days when wind changes were accompanied by strong rise and fall patterns to ascertain the likely development of density currents and ensuing weather. A Doppler radar that was installed at Buckland Park in 2005 will also allow for an increased understanding and identification of wind squalls with the passage of troughs and density currents, however this case study pre-dated its installation.

Summary

Severe winds were recorded across many parts of South Australia on 2 April 2005 associated with the passage of a density current that became established along a pre-frontal trough. An extensive area of dust accompanied the density current, producing significant reductions in visibility.

Key points arising from this event include:

- A low pressure trough formed ahead of a cold front aligned with the western flank of a 1000-500 hPa thermal ridge. A strong temperature gradient existed across the trough boundary with hot

and clear air ahead of the trough producing falling pressure while cooler conditions under a precipitating cloudband following the trough produced rising pressure. A density current formed at the interface between the two air masses and advanced eastwards at a speed greater than that of the initial trough.

- Sharp pressure rises with the onset of the density current produced significant increases in wind speed due to the isobaric wind and momentum changes.
- The density current was long-lived, maintaining its strength and structure as it moved from the west of the State in the early afternoon to the eastern districts in the evening, with the time between the first and last recorded severe wind gusts spanning seven hours.
- Dry lead-up conditions and local bushfires provided ample dust and ash to be lifted with the passage of the density current, causing significant reductions in visibility.
- Internal gravity waves at the head of the density current produced a periodicity in wind speed, pressure and visibility that varied according to the Brunt-Väisälä frequency, with local maxima in wind speed coinciding with local minima in pressure and visibility.
- Numerical weather prediction captured the initial advancement of the pre-frontal trough, however it was unable to simulate the development of the density current.

Acknowledgments

The author wishes to thank supporting staff from the South Australian Regional Office, in particular Alan Cusworth for his encouragement and direction; Graham Cowan and Allan Beattie for their useful insights; and to Bob Schahinger for his assistance in making the pressure tendency charts. Thanks also to Robert Nash, National Climate Centre, Bureau of Meteorology, for providing the temperature analyses. My appreciation is also extended to Dr Andrew MacKinnon, University of Adelaide, for providing the wind profiler data and accompanying background information. And a final thank you to the editors of the *Eyre Peninsula Tribune* and *Whyalla News* for permission to use photographs previously published in their respective newspapers. The individual authors of these and other photographs are credited in the captions and I hasten to forward my appreciation to these people as well. Thank you.

References

- Crook, N.A. 1988. Trapping of low-level internal gravity waves. *J. Atmos. Sci.* 45, 1533–41.
- DPIR 2005. *Crop and Pasture Report March 2005*, Dept. Primary Industry and Resources, SA: http://www.pir.sa.gov.au/pages/agriculture/crop_rep/mar05cpr.pdf, 5–6.
- Eom, J.K. 1975. Analysis of the internal gravity wave occurrence of 19 April 1970 in the Midwest. *Mon. Weath. Rev.*, 103, 217–26.
- Garratt, J.R. 1984. Cold fronts and dust storms during the Australian summer 1982 – 1983. *Weather*, 39, 98–103.
- Kusunoki, K and Eito, H. 2003. Analytical studies of low-level internal gravity waves over the Kanto Plain associated with a stationary front. *Mon. Weath. Rev.*, 131, 236–48.
- Simpson, J.E. and Britter, R.E. 1980. A laboratory model of an atmospheric mesofront. *Q. Jl R. Met. Soc.*, 106, 485–500.
- Sun, J., Burns, S.P., Lenschow, D.H., Banta, R., Newsom, R., Coulter, R., Frasier, S., Ince, T., Nappo, C., Cuxart, J., Blumen, W., Lee, X. and Hu, X-Z. 2002. Intermittent turbulence associated with a density current passage in the stable boundary layer. *Bound. Lay. Met.*, 105, 199–219.